

UV-IR luminosity functions and stellar mass functions of galaxies in the Shapley supercluster core

A. Mercurio, C. P. Haines, P. Merluzzi, G. Busarello, R. J. Smith, S. Raychaudhury, and G. P. Smith

Abstract We present a panchromatic study of luminosity functions (LFs) and stellar mass functions (SMFs) of galaxies in the core of the Shapley supercluster at $z=0.048$, in order to investigate how the dense environment affects the galaxy properties, such as star formation (SF) or stellar masses. We find that while faint-end slopes of optical and NIR LFs steepen with decreasing density, no environment effect is found in the slope of the SMFs. This suggests that mechanisms transforming galaxies in different environments are mainly related to the quench of SF rather than to mass-loss. The Near-UV (NUV) and Far-UV (FUV) LFs obtained have steeper faint-end slopes than the local field population, while the $24\mu\text{m}$ and $70\mu\text{m}$ galaxy LFs for the Shapley supercluster have shapes fully consistent with those obtained for the local field galaxy population. This apparent lack of environmental dependence for the infrared (IR) LFs suggests that the bulk of the star-forming galaxies that make up the observed cluster IR LF have been recently accreted from the field and have yet to have their SF activity significantly affected by the cluster environment.

1 Introduction

Our panchromatic study of LFs in the Shapley supercluster core (SSC), from UV to IR wavebands, aims to investigate the relative importance of the processes that may be responsible for the galaxy transformations examining in particular the effect of the environment through the comparison of LFs in regions with different local densities.

The SSC is constituted by three Abell clusters: A 3558, A 3562 and A 3556, and two poor clusters SC 1327-312 and SC 1329-313.

The target has been chosen since the most dramatic effects of environment on galaxy evolution should occur in superclusters, where the infall and encounter velocities of galaxies are greatest ($>1\,000\text{ km s}^{-1}$), groups and clusters are still merg-

A. Mercurio · G. Busarello · P. Merluzzi
Istituto Nazionale di Astrofisica – Osservatorio Astronomico di Napoli, Italy,
e-mail: mercurio, gianni, merluzzi@na.astro.it

C. P. Haines · S. Raychaudhury · G. P. Smith
School of Physics and Astronomy, University of Birmingham, Birmingham B15 2TT

R. J. Smith
Department of Physics, University of Durham, Durham DH1 3LE

ing, and significant numbers of galaxies will be encountering the dense intra-cluster medium (ICM) of the supercluster environment for the first time. This work is carried out in the framework of the joint research programme ACCESS¹ (*A Complete Census of Star-formation and nuclear activity in the Shapley supercluster*, [7]) aimed at determining the importance of cluster assembly processes in driving the evolution of galaxies as a function of galaxy mass and environment within the Shapley supercluster. We assume $\Omega_M=0.3$, $\Omega_\Lambda=0.7$ and $H_0=70 \text{ km s}^{-1} \text{ Mpc}^{-1}$.

2 UV-IR Luminosity Functions in different environments

We analysed wide field B - and R -band images acquired with the Wide Field Imager on the 2.2 MPG/ESO telescope (Shapley Optical Survey - SOS [6]) and K -band images obtained at the United Kingdom Infra-Red Telescope (UKIRT) with the Wide Field Infrared Camera (WFCAM), covering the whole of the SSC. These data are complemented by NUV and FUV GALEX data, and Spitzer/MIPS $24\mu\text{m}$ and $70\mu\text{m}$ imaging covering essentially the same region ($\sim 2.0 \text{ deg}^2$) as the optical and NIR data. Full details of the observations, data reduction, and the production of the galaxy catalogues are described in [6], [7], and [2] for the optical, NIR and UV/IR images, respectively.

We derive optical and NIR LFs in a 2.0 deg^2 area covering the SSC. In order to investigate the effects of the environment on galaxy properties, in Fig. 1 we show and compared the LFs in three different regions of the supercluster, characterised by high- ($\rho > 1.5$; black points, curves), intermediate ($1.0 < \rho < 1.5$; red), and low-densities ($0.5 < \rho < 1.0 \text{ gals arcmin}^{-2}$; blue) of galaxies. The local density was determined across the R -band WFI mosaic (see [6] for more details). The left and central panels show, respectively the B - and RS -band LFs

The optical LFs cannot be described by a single Schechter function (S) due to the dips apparent at M^*+2 both in B and R bands and the clear upturn in the counts for galaxies fainter than B and $R \sim 18 \text{ mag}$. Instead the sum of a Gaussian and a Schechter function (G+S), for bright and faint galaxies, respectively, is a suitable representation of the data. Furthermore, the slope values becomes significantly steeper from high- to low-density environments varying from -1.46 ± 0.02 to -1.66 ± 0.03 in B band and from -1.30 ± 0.02 to -1.80 ± 0.04 in R band, being inconsistent at more than 3σ c.l. in both bands. Such a marked luminosity segregation is related to the behaviour of the red galaxy population: while red sequence counts are very similar to those obtained for the global galaxy population, the blue galaxy LFs are well described by single S and do not vary with the density (see [6]). This suggests that mechanisms transforming galaxies in different environments are mainly related to the quenching of SF.

In Fig. 1 (right panel), we show the K -band LFs of galaxies in the high- (black), intermediate- (red) and low-density (blue) regions together with their fits with a

¹ <http://www.oacn.inaf.it/ACCESS>

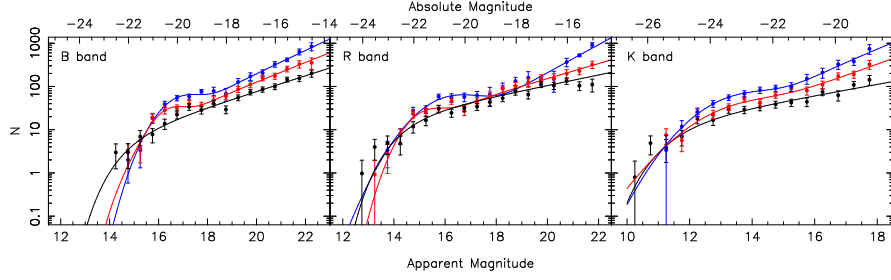


Fig. 1 Galaxies LFs *B*- (left panel), *R*-band (central panel) and *K*-band (right panel) in the high- (black), intermediate- (red) and low-density (blue) environments. Continuous lines represent the G+S best fit for intermediate- and low-density environments and S best fit for high-density regions

Schechter function (same colour code). Although the fit with a single S function cannot be rejected in all the three environments, the LFs suggest a bimodal behaviour due to the presence of an upturn for faint galaxies. To successfully model these changes in slope and to compare our results with our optical LFs, we fit our data with a composite G+S. Moreover, the faint-end slope becomes steeper from high- to low-density environments varying from -1.33 ± 0.03 to -1.49 ± 0.04 , being inconsistent at the 2σ confidence level (c.l.) between high- and low-density regions. The observed trend with environment confirm those observed for the Shapley optical LFs although at lower significance level dramatic for the Shapley optical LFs.

From the GALEX data we obtained NUV and FUV LFs (Fig. 2, left panel), which were found to have steeper faint- end slopes ($\alpha = -1.5 \pm 0.1$) than the local field population ($\alpha = -1.2 \pm 0.1$) at the $\sim 2\sigma$ level, due largely to the contribution of massive, quiescent galaxies at $M_{FUV} \sim -16$. Using the Spitzer/MIPS $24\mu\text{m}$ imaging, we determined the IR LF of the SSC, finding it well described by a single Schechter function with $\log(L_{IR}^*/L_{\odot}) = 10.52^{+0.06}_{-0.08}$ and $\alpha_{IR} = -1.49 \pm 0.04$. We also presented the first $70\mu\text{m}$ LF of a local cluster with Spitzer, finding it to be consistent with that obtained at $24\mu\text{m}$. The shapes of the $24\mu\text{m}$ and $70\mu\text{m}$ LFs were also found to be indistinguishable from those of the local field population (blue squares in Fig. 2 central and right panel). This apparent lack of environmental dependence for the shape of the FIR luminosity function suggests that the bulk of the star-forming galaxies that make up the observed cluster infrared LF have been recently accreted from the field and have yet to have their SF activity significantly affected by the cluster environment. As the SF is quenched via cluster-related processes, the UV and IR emission drops rapidly, taking them off the LFs, reducing its normalization but not affecting its shape.

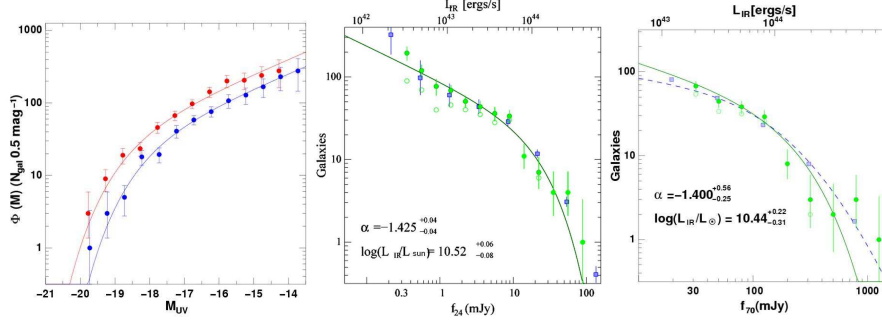


Fig. 2 *Left panel* FUV (blue) and NUV (red) LFs. The solid lines indicate the best-fitting S functions to the data. *Central and right panel:* 24 μm and 70 μm LF (solid green symbols), respectively. In both panels the contribution due to spectroscopically confirmed supercluster members is indicated by open symbols and the best fitting S is indicated by solid green curve. Blue squares represent the field 24 μm LF of [4] in the central panel and in the right panel the field LF of IRAS galaxies from [9], while the blue dashed curve indicates the analytic form of the IRAS field IR LF of [8].

3 The galaxy stellar mass functions

The combined optical and NIR data allow us to derive the distribution of galaxy stellar masses. The sample we analysed is in the magnitude range $10 \leq K \leq 18$ and refers to the $\sim 2 \text{ deg}^2$ area covered by both the SOS and our K -band imaging. The stellar masses of galaxies belonging to the SSC are estimated by means of stellar population models by Maraston ([5]) with a Salpeter initial mass function constrained by the observed optical and infrared colours (see [7] for details). We use the probability that galaxies are supercluster members as derived by [1] following [3] in order to estimate and correct for the foreground/background contamination. We choose that stellar masses of galaxies belonging to the Shapley supercluster contribute to the galaxy SMF according to their likelihood of belonging to the SSC.

In Fig. 3 we show the SMF for the different supercluster environments. Unlike in the case of the optical and NIR LFs no environmental trend is seen in the slope of the SMFs. On the other hand, the M^* increase from low- to high-density regions and the excess of high-mass galaxies remains dependent on the environment. The different behaviours of LF and of galaxy SMF with the environment confirm that the mechanisms transforming galaxies in different environments are mainly related to the quenching of SF rather than to mass-loss.

4 Conclusions

We find that optical and the K -band LF faint-end slope becomes steeper from high- to low-density environments, although the changes in slope are less dramatic at NIR wavebands indicating that the faint galaxy population increases in low-density en-

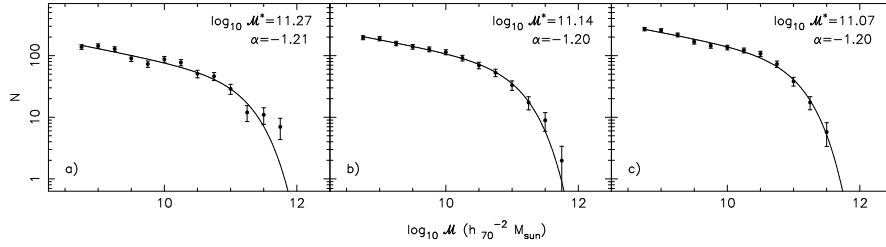


Fig. 3 The mass function of galaxies in the three cluster regions corresponding to high- (panel a), intermediate- (panel b) and low-density (panel c) environments. In the left, central and right panel the continuous line represents the fit to the data. In each panel the best fit value of α and $\log_{10} M^*$ are reported.

vironments. Differently from the LF no environmental effect is found in the slope of the SMFs. On the other hand, the M^* increase from low- to high-density regions and the excess of galaxies at the bright-end is also dependent on the environment. These results seem indicate that the physical mechanism responsible for the transformation of galaxies properties in different environment are mainly related to the quenching of the SF. Moreover, the NUV and FUV LFs obtained have steeper faint-end slopes than the local field population, while the $24\mu\text{m}$ and $70\mu\text{m}$ galaxy LFs for the Shapley supercluster have shapes fully consistent with those obtained for the Coma cluster and for the local field galaxy population. This apparent lack of environmental dependence for the shape of IR luminosity functions suggests that the bulk of the star-forming galaxies that make up the observed cluster infrared LF have been recently accreted from the field and have yet to have their SF activity significantly affected by the cluster environment.

Acknowledgements This work was carried out in the framework of the FP7-PEOPLE-IRSES-2008 project ACCESS. AM acknowledges financial support from INAF-OAC and the JENAM grant to attend the conference.

References

1. Haines C. P., Merluzzi P., Mercurio A., et al., 2006, MNRAS, 371, 55
2. Haines C. P., Busarello, G., Merluzzi P., et al., 2010, MNRAS, arXiv:1010.4323
3. Kodama T., Bower R., 2001, MNRAS, 321, 18
4. Marleau F. R., Fadda D., Appleton P. N., et al., 2007, ApJ, 633, 218
5. Maraston C., 2005, MNRAS, 362, 799
6. Mercurio A., Merluzzi P., Haines C. P., et al., 2006, MNRAS, 368, 109
7. Merluzzi P., Mercurio A., Haines C. P., et al., 2010, MNRAS, 402, 753
8. Takeuchi T. T., Yoshikawa K., Ishii T. T., et al., 2003, ApJL, 587, 89
9. Wang L., Rowan-Robinson M., 2010, MNRAS, 401, 35